Optideneffnet: Deep Learning Framework For Retinal Diseases Prediction

Antara Malakar[1*], Ankur Ganguly[2], Swarnendu Kumar Chakraborty[3]

[1*]*PhD Scholar, Department of Computer Science and Engineering, The Assam Royal Global University, Guwahati*
[2]*Professor, Department of Computer Science and Engineering, The Assam Royal Global University, Guwahati*
[3]*Associate Professor, Department of Computer Science and Engineering, National Institute of Technology, Arunachal Pradesh*

***Corresponding Author:** Antara Malakar*
**PhD Scholar, Department of Computer Science and Engineering, The Assam Royal Global University, Guwahati*

KEYWORDS
Retinal Diseases classification, Deeplearning, Discriminative Gated Recurrent Unit, DenseNet121, EfficientNet, Attention Mechanism.

ABSTRACT
The eye is the primary sensory organ involved in vision. Since some eye conditions might result in blindness, it is important to diagnose and treat them as soon as possible. In ophthalmic diagnostics, it is essential to identify various ocular illnesses from fundus images. On the other hand, subjectivity and mistake arise when ophthalmologists manually detect images. As a result, several automation techniques are developed, however they need to improve in terms of classification accuracy. This work proposes a novel multi-label automated Deep Learning (DL) prediction system called OptiDenEffNet, which can identify various retinal illnesses, as a solution for such challenges. The study begins with an extensive pre-processing step includes label encoding, data cleaning and normalization. The proposed OptiDenEffNet model, which combines many DL blocks, and the Attention Block, which act as feature descriptors, are then used to extract discriminative deep feature representations. Finally, a Discriminative Gated Recurrent Unit (DGRU), a highly developed prediction model is used. This DGRU can provide a probability distribution that precisely predict eye disorders on particular age by incorporating a Softmax layer to its architecture. Extensive tests are conducted on the challenging Ocular Disease Recognition Dataset using Python platform. The proposed model achieves the maximum accuracy of 98.269% and 99.691% in the 70:30 and 80:20 data splits respectively. The results specify that the proposed OptiDenEffNet model works better than state-of-the-art for predict retinal diseases.

Introduction

Processing of visual information requires the human retina. A layer of photosensitive optical nerve tissues is present within the eyeball [1]. The lens focuses light onto the retina, which then generates nerve signals [2]. If proper diagnosis and treatment are not received in a timely manner, eye problems may cause partial or whole vision loss. The onset of vision loss can be stopped with early diagnosis [3] [4]. Visual acuity is typically used to define vision impairment, also known as vision loss. A person with vision impairment has visual acuity of less than 20/40 or 20/60, which is less than the normal value of 20/20. In 2015, it was determined that 1.5 billion of the 7.33 billion persons on the earth have vision impairments. [5].

Blindness is largely caused by retinal illnesses, including glaucoma, age-related molecular degeneration (ARMD), and diabetic retinopathy (DR) [6]. Prompt diagnosis and accurate recovery from these disorders are necessary for the avoidance of vision loss and for timely treatment [7].The intricacy and diversity of retinal pictures, however, might make it difficult for human professionals to precisely and effectively identify and classify retinal illnesses [8]. Thus, the creation of an automated system for classifying retinal diseases with DL or neural network models can greatly improve the speed and accuracy of diagnosis and therapy. A collection of eye disorders known as glaucoma cause damage to an optic nerve [9].In the world, the main causes of blindness include [10]: DR, Cataract, ARMD, myopia, and Glaucoma.

The Optical Coherence Tomography (OCT) is a non-invasive imaging technique that providing high-resolution data across a cross-sectional area [11]. OCT retinal imaging makes it possible to see the different layers of the retina's thickness, structure, and detail [12]. Additionally, OCT makes it possible to see aberrant characteristics and damaged retinal structures when a disease grows in retina. Thus, OCT images are frequently utilized in the medical domain to monitor data in medical imaging before treatment or to identify a variety of illnesses[13].Ophthalmologists have been using retinal OCT images in medical laboratories for many years for looking at the detailed information within the retina

for diagnosis, treatment, and retinal care services [14]. The clinician waits for each phase while manually completing these activities. Therefore, when there are many OCT images, manual analysis takes a long time. This analysis might not be accurate, even in cases where the doctor is quite knowledgeable [15]. This limitation has been addressed by the recommendation of an automated method based on DLwith artificial intelligence.

The advance of DL and computer vision in recent years has developed novel possibilities for automating the classification of retinal disorders. There are still large gaps in classification accuracy, especially in multi-label scenarios where multiple diseases can exist together, despite the encouraging results from various DL techniques. The demand for improved ophthalmic diagnostic capabilities is the motivation behind this research. The increasing number of retinal disorders needs an accurate automated system that can assist doctors in diagnosing and treating these conditions immediately. Despite their potential, existing DL models face several limitations, including difficulty in achieving high predicting and classification accuracy, inability to handle classifications effectively, and a lack of robust generalization across different age groups. To overcome these issues, this work introduces a novel DL framework that is specifically made for retinal disease prediction based on patient's age. Thekey objective of proposed model is to develop an innovative DL system that integrates deep learning blocks and attention mechanism to enhance retinal disease prediction over different age. The primary contributions of this research summarized as follows:

- This study proposes OptiDenEffNet that combines advanced deep learning blocks and attention mechanisms which offers a strong foundation for the classification of retinal diseases.
- This study introduces attention mechanism which focus on relevant features within the input data, improving overall classification performance of model.
- The study employs Discriminative Gated Recurrent Unit (DGRU) that effectively captures sequential patterns in the data, which is crucial for accurately distinguishing between multiple retinal disorders.

The remaining portion of the document is separated into the subsequent themes: In Section 2, the earlier study conducted by other researchers is defined. In Section 3, the proposed methodology is explained. Section 4 discusses the experimentation results of proposed model, and main conclusions are summarized in Section 5.

1. Literature Survey

This section intends to present a summary of the approaches currently used to classify retinal diseases, emphasizing both their advantages and disadvantages. It will also highlight important areas that require additional study.

Choudhary et al. [16] designed a deep CNN with 19 layers, known as the VGG-19 architecture. Transfer learning gives VGG-19 architecture more power. The model is built to be able to identify four different retinal diseases based on its ability to learn from a sizable collection of OCT images.

Khan et al. [17] suggested DL-based automatic technique that uses OCT images to identify and categorize retinal disorders. Transfer learning was used to obtain the features on three pretrained models: ResNet-50, InceptionV3, and DenseNet-201, after some initial adjustments based on the dataset's characteristics.

Stanojević et al. [18] designed to investigate the many applications of DL more especially, the use of CNN in retinal disorders. Several architectures were investigated during the research, including AlexNet, VGG, Inception, and residual networks. Based on the Inception architecture, the CNN demonstrated the highest level of success in the classification. However, as models based on CNNs with more layers converge more slowly, this study's execution time is limited.

Shoukat et al. [19] established accurate DL-based automatic method for glaucoma identification in its early stages. The proposed model uses ResNet-50 architecture and fundus images to diagnose early-stage glaucoma. The CNN model was trained on sizable dataset of varied fundus images by utilizing the gray channels included in the images as well as the data augmentation technique.

Albelaihi and Ibrahim [20] designed DL model with multiclassification to diagnose and identify four different diabetic eye conditions. In this work, the performances of five architectures are examined:

ResNet152V2 + GRU, ResNet152V2 + Bi-GRU, VGG16, EfficientNetB0, and ResNet152V2. An extensive number of tests and outcomes utilizing fundus images from various sources showed that the EfficientNetB0 model performed better than other five suggested models.

Hemalakshmi et al. [21] presented hybrid SqueezeNet-vision transformer model that captures both local and global features of OCT images for more precise classification while lowering computational complexity. The strengths of both vision transformer and squeezenet were combined in this concept. The OCT2017 dataset was used for training, testing, and validation in the proposed model, which performs multiclass and binary classification.

Hassan et al. [22] suggested DL-based method for detecting CSRs that makes use of fundus photography and OCT imaging. DarkNet and DenseNet networks are trained using both datasets once these manually enhanced input photos have been classified. However, this study required extra time due to the experiments' use of technology that was only partially compatible.

Zia et al. [23] presented a method that leverages the properties of an eye image to concurrently detect multiple disorders, including cataract, glaucoma, and diabetic retinopathy. This method is based on an enhanced deep learning algorithm called SqueezeNet. In this investigation, SqueezeNet has an extra layer, and the Bottleneck Attention Module (BAM) was used. Additionally, the suggested scheme is built on an effective pre-trained SqueezeNet architecturewhich computes quickly. However, training time of suggested approach must be reduced to improve the model performance.

Nguyen et al. [24] developed an automated system to improve and process a 4697-image collection. These networks properly depict and evaluate medical pictures by applying transfer learning from pre-trained models and layer-wise feature extraction. ResNet152 is the most efficient and accurate of the five models that were assessed; the other models are Vision Transformer, InceptionResNetV2, RegNet, and ConVNext.

George et al. [25] have proposed the categorization and severity analysis of retinal and choroidal disorders in OCT images to be accomplished by two-stage CNN model. The suggested approach was able to recognize aberrant diseases including Drusen, macular edema, and pachyporoid disorders. For the first classification, a modified version of VGG16 architecture was employed. After then, a refined CNN with the similar architecture was used to assess the severity of pachchoroid illnesses. In addition, the authors evaluated the degree of macular edema using UNet architecture.

Research gaps are still quite large even with improvements in automated techniques for predicting and categorizing retinal diseases. The predicting and classification accuracy of existing algorithms is significantly impacted by the lack of comprehensive processing methods that improve quality. The diagnostic capability of traditional deep learning models is limited due to their inability to capture adequate feature representation. In order to increase feature extraction, this studyproposes the OptiDenEffNet model, which combines sophisticated preprocessing methods, attention mechanism, and DGRU to improve classification and prediction performance. In order to close these gaps and potentially enhance treatment results, the proposed structure seeks to offer a more accurate and reliable method for predictingeye diseasesacross different age groups.

2. Proposed Methodology

This paper proposes novel OptiDenEffNet that designed for classifyvarious retinal disorders based on age. This study involves three stages: preprocessing, Feature extraction, and classification. Initially, the preprocessing techniques are applied to preprocess the raw data. The preprocessing methods used in this study include data cleaning and min max normalization. Then the preprocessed data is forward to proposed framework for feature extraction and classification. The developed system is the hybrid approach of EfficientNet and DenseNet 121 and additionally it includes attention mechanism and DGRU to enhance feature extraction and classification process. An effective tool for identifying sequential dependencies in the data is the Discriminative Gated Recurrent Unit (DGRU), which is used in the classification step. The DGRU provides a probability distribution for identifying distinct eye diseases by adding a Softmax layer, allowing for a more complex comprehension of the relationships between various diseases. The pipeline framework of proposed method is shown in Figure 1.

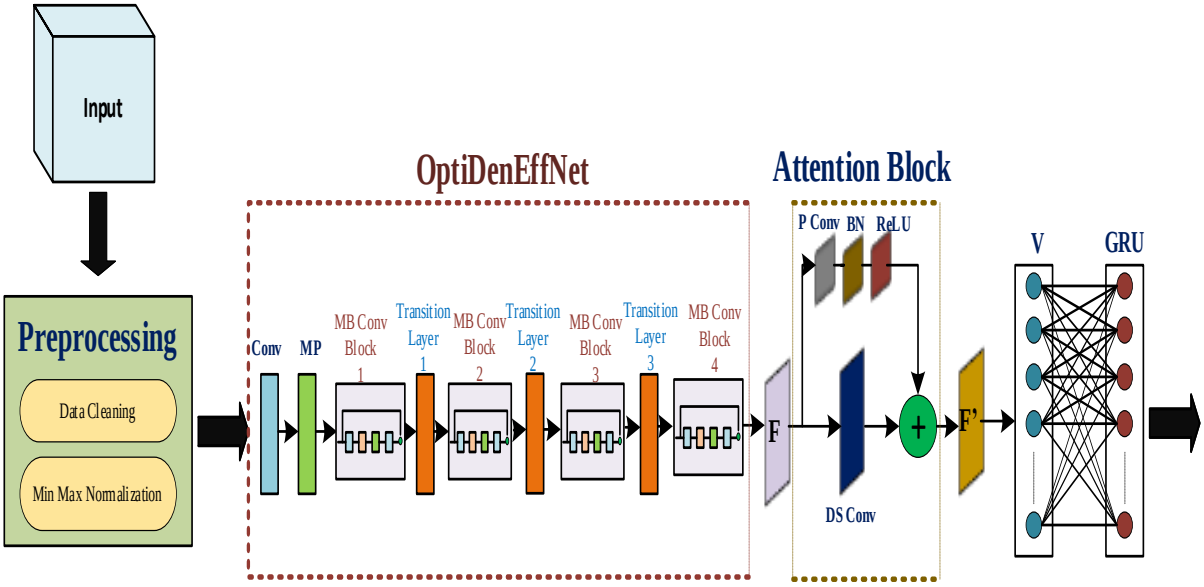

Figure 1. Overview of proposed framework

2.1. Preprocessing

Initially, the raw data from dataset is applied for preprocessing. This work employs two methods for preprocess the input data: Label encoding, Data cleaning and normalization.

Label Encoding is an important pre-processing step and it is a technique that is used to convert categorical columns into numerical ones so that they can be fitted by models which only take numerical data. The process of identifying and eliminating errors, inconsistencies, and inaccuracies from dataset is called data cleaning, sometimes referred to as data cleansing or data scrubbing. This important stage is required for analysis and decision-making to be effective.A data preprocessing method called normalization is used to convert the dataset's numeric column values to a common scale without erasing or distorting information about the ranges of values. Normalized data makes it easier for the model to learn the patterns by ensuring that each feature contributes equally to the model training process. This study uses min max normalization method to normalize the input data.

Min-max normalization scales the data between a specified range, usually 0 to 1. The formula for calculating the Min-Max Scaling is given in Eqn. ():

$$Y_{norm} = \frac{(Y - Y_{min})}{(Y_{max} - Y_{min})}$$

The input data after applying data cleaning and min max normalization is forward to proposed OptiDenEffNet technique for extract the features from input data.

2.2. Feature Learning using OptiDenEffNet model

This study proposes OptiDenEffNet model for classifying eye disorder effectively. The proposed model is developed by combiningEfficientNet and DenseNet 121 models. EfficientNet uses Mobile Inverted Bottleneck (MBConv) layers, which are a combination of inverted residual blocks and depth-wise separable convolutions (DS Conv). The convolutional layer of DenseNet is replaced by MBConv layer of EfficientNet. The hybrid strategy that combines EfficientNet and DenseNet-121 in a multi-label DL framework for the categorization of retinal diseases efficiently makes use of the advantages of both architectures. Better gradient flow and more accurate feature learning are made possible by DenseNet-121, which also improves feature reuse and addresses the vanishing gradient issue. EfficientNet is well-known for its efficient scaling and decreased processing requirements. This combination produces faster training convergence, stronger resistance to overfitting, and increased prediction accuracy. Computational efficiency is increased by adopting EfficientNet's MBConv layer for DenseNet's convolutional layer. Large datasets require careful processing, and this integration significantly

decreases resource consumption without sacrificing performance. The MBConv layer uses depthwise separable convolutions to improve model generalization and mitigate overfitting by allowing for better feature extraction with fewer parameters. Its adaptive scaling maximizes learning dynamics and accelerates training and inference periods. The model is more appropriate for clinical applications where predict eye diseases from age, which also improves accuracy. Incorporating the MBConv layer enhances predicting efficacy and durability in identifying various retinal diseases based on patient's age.

2.2.1. MB Conv Block

MBConv is the fundamental building block of the EfficientNet architecture, featuring squeeze and excitation optimization. A specific type of residual block called an MBConv Block is utilized for image models that, in order to maximize efficiency, have an inverted structure. An MBConv is intended to increase the efficiency and adaptability of CNNs. The DS Conv is used by MBConv to achieve this. The channels will initially be widened using a point-wise convolution (conv 1x1). The number of parameters is then significantly reduced by using a 3x3 depth-wise convolution. Lastly, the number of channels will be reduced using a 1x1 convolution, allowing the beginning and end of the block to be added.A typical residual block has a structure that alternates between being broad, narrow, and wide based on the number of channels. 1x1 convolution is used to reduce the vast number of channels in the input. The number of channels is then increased by employing 1x1 convolution to add input and output. On the other hand, an Inverted Residual Block takes narrow -> broad -> narrow path, which accounts for the inversion. First, 1x1 convolution is used to broaden the input data. The number of parameters is then drastically decreased by applying a 3x3 depthwise convolution. Lastly, the number of channels is reduced via 1x1 convolution, allowing input and output to be combined.
The Squeeze and Excitation (SE) block is a building block used by CNNs to perform dynamic featurewise recalibration, which enhances the interdependencies between the features by dynamically assigning high weight to the most important features rather than evenly weighting all of the features. The SE block is applied by EfficientNet in conjunction with the MBConv block, provides the following structure.

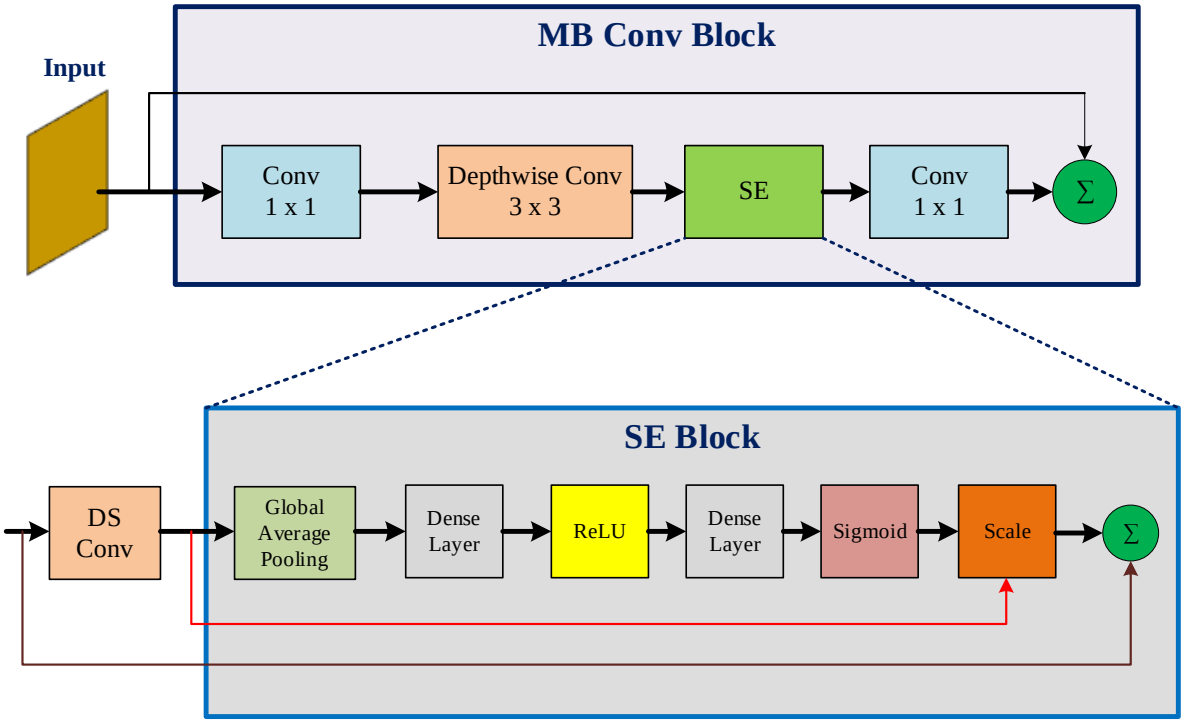

Figure 2. Structure of MB Conv Block

2.2.2. Transition Layer

A transition layer is employed to regulate the model's complexity. Their two primary functions are to decrease the quantity of feature maps and to downsample the feature maps' spatial dimensions. This

contributes to keeping the network small and computationally efficient. The components of a typical transition layer are average pooling, 1x1 convolution, and batch normalization. The 1x1 convolution is used to reduce the number of features. Additionally, it uses average pooling to reduce the dimension in half with a stride of 2.
The prediction performance can be enhanced by adding attention mechanism after feature extraction. Therefore, this study introduces Depthwise Separable Convolution (DSConv) based attention block to improves prediction performance.

2.3. Attention Block

The attention block generates unique feature attention maps by utilizing features that are taken from the OptiDenEffNet. The feature maps Facquired from OptiDenEffNet network are transferred into F' using 3 x 3 DSConv and 1 × 1 Pointwise Convolution. DSConv significantly outperforms conventional convolutions in neural networks, increasing representational efficiency with fewer parameters and less computing overhead. The Batch Normalize layer processes the PConv layer's output to reduce overfitting and speed up model convergence. This is followed by augmenting the model's non-linearity with ReLU function. The feature maps obtained from both DSConv and Pconv can be combined in the following manner to obtain the final feature representations F' generated from the attention block:

$$F' = concat\left(DSconv(F), ReLU\left(BN\left(Pconv(F)\right)\right)\right) \quad (3)$$

Where, the terms $concat$ stands for concatenation. The goal of the attention block is to identify disease by highlighting pertinent characteristics and eliminating distracting features. The process is carried out as follows:

- An array of feature maps is created from an input datausing convolutional layers in the attention block. These maps extract several levels of abstraction from source data.
- The attention mechanism generates attention maps that, in terms of relevance, highlight different features within the feature maps. The process of training involves learning these maps.

The generated relevant feature map using attention block is applied to DGRU for predicting eye diseases.

2.4. Prediction usingDiscriminative Gated Recurrent Unit

A type of RNN that can handle long-range patterns in the input data and recognize sequential relationships is the GRU. The reset and update gates that GRUs employ regulate the amount of historical data that is transmitted and the amount of current input that is integrated. This enables the model to handle sequences effectively while retaining relevant data. The primary objective of a DGRU is to identify the most important characteristics that set one class distinct. It focuses on patterns that improve classification performance rather than generatively modeling the input data. As opposed to standard sequence models, which aim to only forecast the next value in a series, discriminative GRU models aim to classify the sequence or a portion of it.

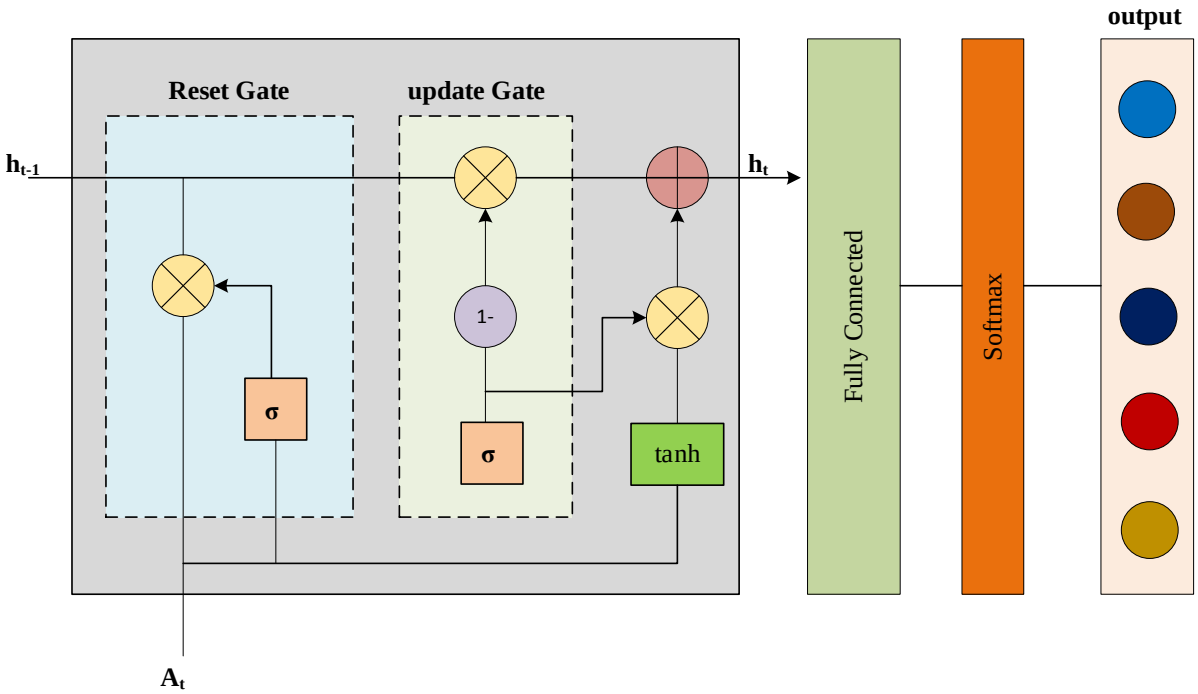

Figure 3. Architecture of DGRU

A reset gate and an update gate make up a GRU's architectural design. The information passing across the cell is accepted and rejected by the two gates. The reset gate determines the amount of historical data to be erased. A sigmoid activation function (σ) is used to carry out this decision. The output of the sigmoid represented as s_t. In case the sigmoid function value is 1, the data will be incorporated into the GRU algorithm; in case it is 0, the data cannot be incorporated into the GRU algorithm. The reset gate's inputs are the current input (A_t) and the previous hidden state (h_{t-1}). The update gate determines what data will be modified to convey a future state. The update gate is therefore reliant on a very fundamental feature of the previous state.

The data will be entered into the GRU algorithm if the sigmoid function value is 1; if the sigmoid function value is 0, the data cannot be entered into the GRU algorithm. The current input (A_t) and the prior hidden state (h_{t-1}) serve as the reset gate's inputs. The information that will be updated to transmit a future state is determined by the update gate. As a result, the update gate is dependent on a very basic aspect of the prior state. A sigmoid activation function is also included in the update gate to update the cell state. The range of this function is 0 to 1. After multiplying the sigmoid's output, g_t, by the $tanh$ function, a new cell state $\hat{h}_t$ is produced. The $tanh$ values range from -1 to 1. The current cell state C_t, where h_t is the current hidden state output of the current cell, is increased by the multiplication process. Eqns. (4) and (5) are used to determine the reset gate and update gate, respectively.

$$s_t = \sigma(\omega_s[h_{t-1}, A_t]) \quad (4)$$

$$g_t = \sigma\left(\omega_g[h_{t-1}, A_t]\right) \quad (5)$$

In this case, ω_s and ω_g stand for weight of reset and update gates respectively.

$$h_t = (1 - s_t) \times h_{t-1} + g_t \times \hat{h}_t \quad (6)$$

The weights will be learned throughout the training period. Furthermore, Eqn. (6) is used to determine the h_t of the GRU cell.

In DGRU, non-linear activation and an extra weight matrix are used to improve class discrimination. It can be calculated as following expression:

$$h_t^D = ReLU(\omega_d \cdot h_t + b_d) \quad (7)$$

Where, b_d denotes bias term, ω_d represents discriminative weight, $ReLU$ is activation function to introduce non-linearity and improve discrimination.
The final hidden state is sent to a softmax layer for classification following the DGRU's processing of the sequence data. A probability distribution covering the five classes (diabetic retinopathy, cataracts, glaucoma, AMD, and myopia) is provided by the softmax layer:

$$\hat{R} = Softmax(\omega_z \cdot h_T^D + b_z) \quad (8)$$

Where, b_z denotes bias term for the softmax layer, h_T^D stands for discriminative hidden state at the last time step, ω_z represents output weight matrix, and $\hat{R}$ signifies predicted probabilities for each class.
The optimization of the parameters (weights and biases) of DGRU is critical to its performance. Local minima or saddle points may be problematic for traditional optimization techniques where temporal relationships are taken into consideration.To overcome these issues, this study introduces SaLOA strategy to optimize the parameters of DGRU. LOA is helpful in avoiding frequent errors such as premature convergence and local minima and self adaptive approach also introduced into LOA to further enhance the performance of traditional LOA. The mathematical strategy of SaLOA is described in subsequent section.

2.4.1. Self-Adaptive Lyrebird Optimization Algorithm

This section describes the motivation behind the suggested Lyrebird Optimization Algorithm (LOA) and presents its mathematical modeling for usage in optimization tasks.

A. Mathematical Modelling of SaLOA

The LOA technique, which is covered below, was created using mathematical modeling of this lyrebird tactic in times of risk.

B. Initialization

The LOA method is a population-based metaheuristic algorithm in which the population is made up of lyrebirds. The population of the algorithm is made up of all LOA members, and it can be formally represented as a matrix using Eqn. (9). Eqn. (10) is used to initialize the initial positions of LOA members at random in the problem-solving space.

$$P = \begin{bmatrix} P_1 \\ \vdots \\ P_i \\ \vdots \\ P_N \end{bmatrix}_{N\times m} = \begin{bmatrix} p_{1,1} & \cdots & p_{1,d} & \cdots & p_{1,m} \\ \vdots & \ddots & \vdots & \iddots & \vdots \\ p_{i,1} & \cdots & p_{i,d} & \cdots & p_{i,m} \\ \vdots & \iddots & \vdots & \ddots & \vdots \\ p_{N,1} & \cdots & p_{N,d} & \cdots & p_{N,m} \end{bmatrix}_{N\times m} \quad (9)$$

$$p_{i,d} = LB_d + Rand \cdot (UB_d - LB_d) \quad (10)$$

Where, p represents the number of lyrebirds, m indicates the number of decision variables, $Rand$ denotes a random number in the interval [0,1], P_i is the i^{th} LOA member (candidate solution), P is the LOA population matrix, $p_{i,d}$ is the d^{th} dimension in search space (decision variable), LB is the lower bound and UB is the upper bound of the d^{th} decision variable.
It is possible to assess the problem's objective function by taking into account that every member of the LOA represents a potential solution to the issue. The values for the goal function are therefore available and equal to the number of population members. Equation (11) states that a vector can be used to represent the set of evaluated values for the problem's objective function.

$$O = \begin{bmatrix} O_1 \\ \vdots \\ O_i \\ \vdots \\ O_N \end{bmatrix}_{N\times 1} = \begin{bmatrix} O(P_1) \\ \vdots \\ O(P_i) \\ \vdots \\ O(P_N) \end{bmatrix}_{N\times 1} \quad (11)$$

Where, the evaluated objective function based on i^{th} LOA member is denoted by O_i, and the vector of evaluated objective function is represented by$O$.
The useful criterion for assessing the caliber of the potential solutions is the evaluated values for the objective function. This means that the best candidate solution, or the best LOA member, corresponds to the best evaluated value for the objective function, and the worst candidate solution, or the worst LOA member, corresponds to the worst evaluated value for the objective function. The best candidate solution should also be updated based on the comparison of the objective function value, taking into account that the position of the lyrebirds in the problem-solving space is updated in each iteration.
The position of the population members is updated in each iteration of the SaLOA technique based on the mathematical modeling of the lyrebird strategy when it detects danger. The two phases of the population update process are (i) hiding and (ii) escape, based on the lyrebird's decision in this scenario. Equation (12) simulates the lyrebird's decision-making process in the LOA design when it must select between hiding and escaping from danger.

$$Updated\ process\ of\ P_i : \begin{cases} based\ on\ phase\ I\ ;\ R_p \le 0.5 \\ based\ on\ phase\ II\ ;\quad else \end{cases} \tag{12}$$

Where, R_p denotes random number ranges between 0 and 1.

C. Exploration: Escaping Strategy

The model of the lyrebird's escape from the danger position to the safe areas is used to update the population member's position in the search space during this phase of LOA. The lyrebird's capacity to explore new locations in the problem-solving space and make large positional changes after moving to a safe place is indicative of LOA's global search exploration capability. The positions of other population members with higher objective function values are regarded as safe areas for each member in the LOA design. Eqn. (13) can therefore be used to find the set of safe regions for each LOA member.

$$A_i = \{P_k, O_k < O_i (k \in 1,2, \dots N)\}\ ;\ i = 1,2, \dots N \tag{13}$$

Where, A_i represents the set of safe areas for the i^{th} lyrebird, and P_k denotes the k^{th} row of the P matrix, which has a higher objective function value (i.e., O_k) than the i^{th} LOA member.
The lyrebird appears to randomly flee to one of these safe havens in the LOA design. Eqn. (14) is used for each LOA member to determine a new position based on the lyrebird displacement modeling completed in this step. The new position then replaces the prior position of the relevant member in accordance with Eqn. (15) if the value of the objective function is improved.

$$p_{i,j}^{new\,1} = p_{i,j} + R_{i,j} \cdot \left(SA_{i,j} - H_{i,j} \cdot p_{i,j}\right) \tag{14}$$

$$P_i = \begin{cases} P_i^{new\,1}, & O_i^{new\,1} \le O_i \\ P_i\ , & else \end{cases} \tag{15}$$

Where, $P_i^{new\,1}$ represents the new position determined for the i^{th} lyrebird based on escaping strategy of the proposed LoA, $p_{i,j}^{new\,1}$ is its j^{th} dimension, $O_i^{new\,1}$ is its objective function value, and $R_{i,j}$ are random values in the interval [0, 1]. $SA_{i,j}$ is the chosen safe area for the ith lyrebird. $H_{i,j}$ are numbers that are arbitrarily chosen as 1 or 2.

D. Exploitation: Hiding Strategy

The population member's position is updated in the search space during this phase of LOA in accordance with the lyrebird's modeling technique to conceal itself in the vicinity of a safe region. The ability of the lyrebird to leverage LOA in local search is demonstrated by its ability to move with little steps and accurately examine its surroundings to find a good hiding place. In LOA design, a new position is determined for each LOA member using Eqn. (16), which is based on the modeling of the lyrebird's migration towards the nearby suitable region for concealment. In the event that this new position increases the value of the objective function as determined by Eqn. (17), the relevant member's prior position is replaced.

$$p_{i,j}^{new\,2} = p_{i,j} + \left(1 - 2R_{i,j}\right) \cdot \frac{UB_j - LB_j}{t} \quad (16)$$

$$P_i = \begin{cases} P_i^{new\,2}, & O_i^{new\,2} \le O_i \\ P_i\ , & else \end{cases} \quad (17)$$

Where, t denotes the iteration counter, $O_i^{new\,2}$ is the objective function value, $P_{i,j}^{new\,2}$ is the new position computed for the ith lyrebird based on the concealing strategy of the suggested LOA, and $p_{i,j}^{new\,2}$ is itsj^{th} dimension.
The updated equation of LOA is expressed as follows:

$$P_{new} = p_{i,j} + P_{gbest} + \left(\frac{UB - LB}{t}\right) \quad (18)$$

Conventional LOA might have slow convergence or become trapped in local minima due to issues with either over exploration or exploitation. Therefore, this study introduced self adaptive strategy into LOA to improve the performance. By introducing random and oscillating inertia weights, the behavior of the algorithm can be adjusted dynamically. While oscillating inertia weights modify the exploration-exploitation balance at various stages of optimization, random inertia weights contribute to the preservation of diversity in the search process. The updated SaLOA can be expressed as following Eqn. (19).

$$P_{new} = p_{i,j} + W_1 * P_{gbest} + W_2 * \left(\frac{UB - LB}{t}\right) \quad (19)$$

Where, W_1 represents random inertia weight and W_2 denotes oscillating inertia weight. These two weighted parameters are used to adjust global best and local best solutions of LOA. The mathematical formula of W_1 and W_2 are expressed in Equations (20) and (21) respectively.

$$W_1 = 0.5 + \frac{Rand}{2} \quad (20)$$

$$W_2 = \left(\frac{w_{min} + w_{max}}{2}\right) + \left(\frac{w_{min} - w_{max}}{2}\right) cos\left(\frac{2\pi t}{T}\right) \quad (21)$$

The SaLOA strategy balances exploration and exploitation (concentrating on the best options), which aids in fine-tuning the parameters of DGRU. Through effective DGRU parameter optimization, the SaLOA improves the model and guarantees robust generalization, faster convergence, and higher classification performance across noisy, large-scale retinal image data. The model becomes more clinically relevant and practical for real-world applications as a result of this optimization strategy, which directly improves the multi-label classification of retinal disorders' accuracy and reliability.

2.5. Loss Function

The objective of this study is to developed deep learning network that can predicteye disorders on age. The objective is to maximize the model's capacity to accurately identify each type of retinal diseases while minimizing classification mistakes. The most appropriate loss function to optimize the prediction task is Binary Cross-Entropy Loss function. The loss function is defined as follows:

$$L = -\left[Z \cdot log\left(\hat{Z}\right) + (1 - Z) \cdot log\left(1 - \hat{Z}\right)\right] \quad (22)$$

Where, Z stands for actual data,$\hat{Z}$signifies predicted probability.
The OptiDenEffNet model can predict the correct disease class for each fundus image more accurately by minimizing this loss, which improves diagnostic accuracy and leads to better clinical results.

3. Results and Discussion

In this section, the developed model's performance is assessed, and the results of the proposed design are compared with those of several other models that are already in use.

3.1. Dataset Description

The study uses Ocular Disease Recognition dataset [26] for evaluate the performance of proposed model. An organized ophthalmic database called Ocular Disease Intelligent Recognition (ODIR) has five thousand patient records, including age, color fundus images of the left and right eyes, and physician diagnostic keywords. The purpose of this dataset is to depict a "real-life" set of patient data that Shanggong Medical Technology Co., Ltd. gathered from several Chinese hospitals and medical facilities. These institutions use a variety of cameras on the market, including Canon, Zeiss, and Kowa, to take fundus photos, which produces images with different resolutions. This dataset includes corresponding metadata of Ocular Disease and this metadata is applied to model to predict age related eye diseases. The dataset includes following eight classes: Normal (N), Diabetes (D), Glaucoma (G), Cataract (C), Age related Macular Degeneration (A), Hypertension (H), Pathological Myopia (M), Other diseases/abnormalities (O)

3.2. Experimental Setup

Python 3.10 was used to conduct all of the experiments on hardware consisting of an Intel(R) Core (TM) i6-8100 CPU running at 3.60GHz with 8.00 GB of RAM. According to the 70:30 instructions, 70% of the data was initially set aside for training and 30% for testing. Following that, 80% of the data was used for training and 20% was used for testing the classifiers, in accordance with the 80:20 rule.The classification process of proposed model was carried out with mini-batch size of 32 using categorical cross-entropy loss function. The proposed model with 60 epochs is developed using Adam, the default optimizer. The test dataset was used to evaluate the results using common performance assessment metrics like accuracy, sensitivity, and specificity.

3.3. Performance Metrics

The performance of model was evaluated in this study using the following metrics:Accuracy, Mean Squared Error (MSE), Root Mean Squared Error (RMSE), Mean Absolute Percentage Error (MAPE), Mean Absolute Error (MAE), and R-squared.The description of each evaluation metrices are described below:

(i) Accuracy: It measures the proportion of correctly predicted instances out of the total instances.

$$Accuracy = \frac{No.of\ correct\ \ prediction}{Total\ \ No.of\ prediction} \quad (23)$$

(ii) R-square: This matric demonstrates the extent to which the independent factors account for the dependent variable's variability.

$$R^2 = 1 - \frac{\sum\left(X_i - \hat{X}_i\right)^2}{\sum(X_i - \bar{X}_i)^2}$$

Where, X_i denotes actual value, $\hat{X}_i$ specifies predicted value, $\bar{X}_i$ indicates mean of actual values.

(iii) MSE: It is a mean of squared discrepancy between actual and anticipated values.

$$MSE = \frac{1}{M}\sum_{i=1}^{M}\left(P_i - \hat{P}_i\right)^2 \quad (23)$$

Where, M represents number of data points, P_i and $\hat{P}_i$are denotes actual and predicted value.

(iv) RMSE: It is the square root of MSE. It computes the error's standard deviation.

$$RMSE = \sqrt{\frac{1}{M}\sum_{i=1}^{M}\left(P_i - \hat{P}_i\right)^2} \quad (24)$$

(v) MAE: It is the average of an absolute deviations between initial and anticipated values.

$$MAE = \frac{1}{M}\sum_{i=1}^{M}\left|P_i - \hat{P}_i\right| \quad (25)$$

(vi) MAPE: The percentage error between the actual and projected values is measured by MAPE.

$$MAPE = \frac{1}{M}\sum_{i=1}^{M}\frac{|P_i - \hat{P}_i|}{|P_i|} \times 100\% \quad (26)$$

3.4. Performance of proposed model in prediction

This section discusses the accuracy of disease predictions and displays the model's performance across six age groups, with a particular emphasis on the age-related relationship to the occurrence of certain health conditions. Accurate prediction of age-related diseases is essential for timely diagnosis and efficient treatment of a variety of medical illnesses. This study employs a model to determine the probability of eight distinct diseases across a range of age groupsfrom 18 to 100. The age is divided into six groups to predict the various diseases over different age group. The model highlights the patterns and trends of disease prevalence in different stages of life in an effort to shed light on how age affects the prediction accuracy for certain diseases. Table 1 depicts the evaluation results proposed model on predicting diseases based on several age groups.

Table 1. Accuracy of disease prediction based on age

Age	N	D	G	C	A	H	M	O
18-25	0.8625	-	0.9618	-	-	-	-	0.9265
26-35	0.8962	0.9339	0.9765	-	0.9864	-	0.9682	0.9382
36-45	0.9262	0.9665	0.9886	-	-	-	-	0.9781
46-60	0.9256	0.9326	-	0.9617	0.9816	-	0.9651	0.9565
61-80	0.8853	0.9156	-	0.9582	0.9654	0.9284	0.9518	0.9569
81-100	0.9264	0.9339	0.9695	0.9591	0.9661	-	0.9518	0.9453

The proposed model predicts N, G, and O cases with accuracy of 0.8625, 0.9618, and 0.9265 respectively with good accuracy in the 18–25 age group. Diseases including D, C, A, H, and M classes are not predicted by the model for this age group, suggesting that these problems are not common in younger people, which is consistent with general clinical observations. The model predicts N, D, G, A, M, and O classes with accuracy of 0.8962, 0.9339, 0.9765, 0.9864, 0.9682, and 0.9382 respectively for those between the ages of 26 and 35. In this age range, there are no projections for either H or C cases, which may be because these disorders often show symptoms later in life. For 36-45 age group, the accuracy is still very good for all anticipated diseases. The accuracy of the predictions for cases of N is 0.9262, D is 0.9665, G is 0.9886, and O is 0.9781. This age group currently does not have projections for cataract, age-related macular degeneration, hypertension, or pathological myopia due to their lesser prevalence at this stage of life.

Predictions for 46-60 age range also include additional illnesses like cataracts. High accuracy is achieved by proposed model for the following conditions: N = 0.9256, D = 0.9326,O = 0.9565, M = 0.9651, C = 0.9617, and A = 0.9816. Despite the possibility of their happening, glaucoma and hypertension are not expected in this age group.The model continues to perform effectively in the age range of 61 to 80 years old, accurately predicting the following: N=0.8853, D=0.9156, H=0.9284, M=0.9518, O=0.9569, C=0.9582, and A=0.9654. The model shows consistent performance across most diseases for 81-100 age group. The following are the accuracy of classes in this age group: N=0.9264, D=0.9339, G=0.9695, C=0.9591, A=0.9661, M=0.9518, and O=0.9453 are among the conditions for which predictions are accurate.The model is successful in predicting diseases based on age group, according to this analysis. The performance of accuracy of proposed model on predicting diseases across six age groups are illustrated in Figure 4.

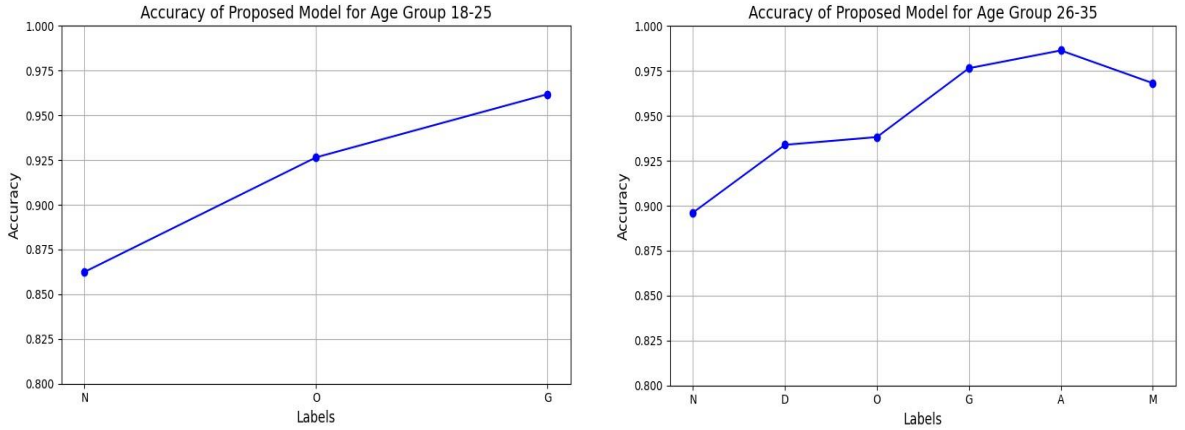

(a) Age group 18 - 25

(b) Age group 26 - 35

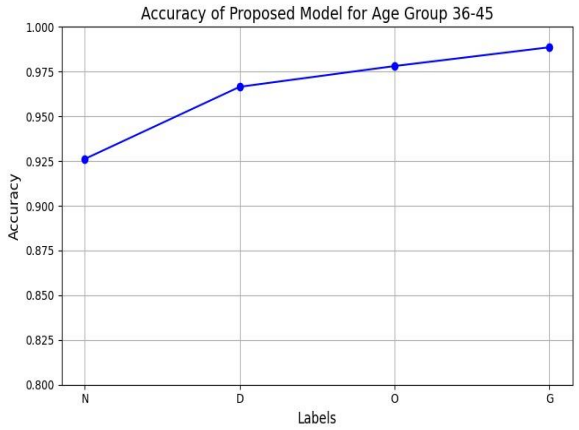

(c) Age group 36 - 45

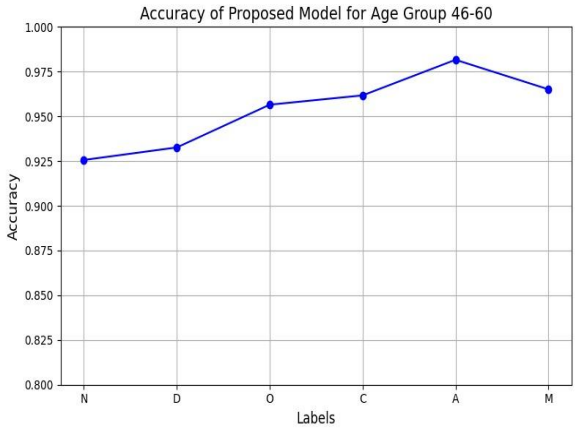

(d) Age group 46 - 60

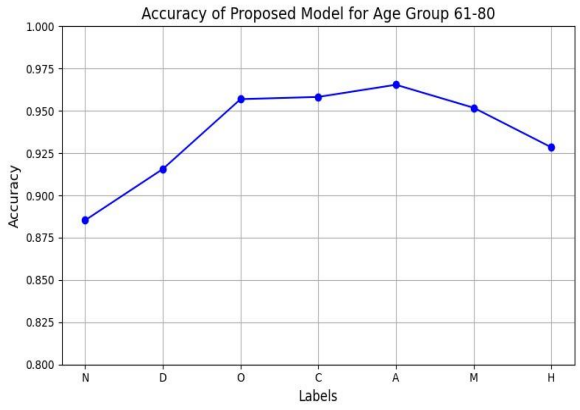

(e) Age group 61 - 80

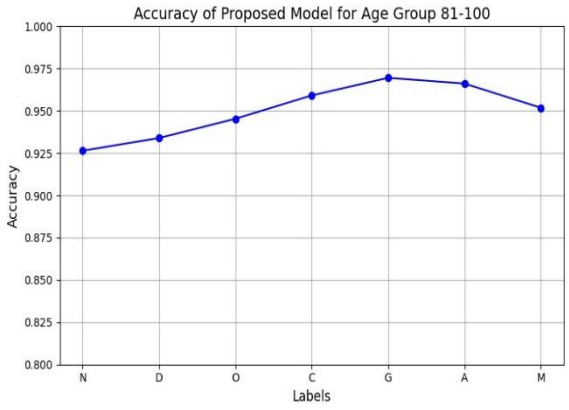

(f) Age group 81 - 100

Figure 4. Accuracy of proposed model in disease prediction based on age group

3.5. Performance and Comparative Analysis

This section evaluates the developed OptiDenEffNetmodel as well as some existing models that are described in literature section. AlexNet [18], VGG 16 [20], ResNet 152 [24], and UNet [25]are the existing models were evaluated to compare the performance of proposed model. Table 2 shows the evaluation results when dataset is splitted in the basis of 70:30 rule and Table 3 depicts the outcomes when the 80:20 data is applied.

Table 2. performance of proposed and existing models based on 70:30 data split

	Accuracy	R-square	RMSE	MSE	MAPE	MAE
VGG-16	94.324	94.042	0.2858	0.3149	0.3347	0.2864
ResNet152	95.185	95.503	0.3019	0.3491	0.3284	0.2616
UNet	96.394	96.831	0.3184	0.2918	0.2774	0.2318
AlexNet	96.928	96.106	0.2994	0.2658	0.2658	0.2568
Proposed	98.269	98.442	0.2456	0.2418	0.2214	0.2147

Table 3. performance of proposed and existing models based on 80:20 data split

	Accuracy	R-square	RMSE	MSE	MAPE	MAE
VGG-16	95.051	95.283	0.2735	0.3026	0.3176	0.2769
ResNet152	96.624	96.213	0.2896	0.3129	0.3028	0.2491
UNet	97.031	97.615	0.3009	0.2792	0.2619	0.2293
AlexNet	97.688	97.815	0.2719	0.2529	0.2519	0.2352
Proposed	99.691	99.085	0.2319	0.2329	0.2064	0.1958

The Accuracy metric quantifies how accurately the model classifies retinal disorders overall. The proposed OptiDenEffNet model performs better than any other model in both data splits. The OptiDenEffNet obtains an accuracy of 98.269% for the 70:30 split, which is substantially higher than other existing models such as ResNet152, VGG-16, AlexNet, and UNet. Again, the OptiDenEffNet model demonstrates even greater performance with an accuracy of 99.691% in the 80:20 split. The aforementioned results of proposed model demonstrating reliable and steady performance across various data splits. Due to its sophisticated feature learning and application of DGRU, the proposed OptiDenEffNet has the better capacity to accurately predict a retinal disorder on specific age. The accuracy analysis is displayed in Figure 5.

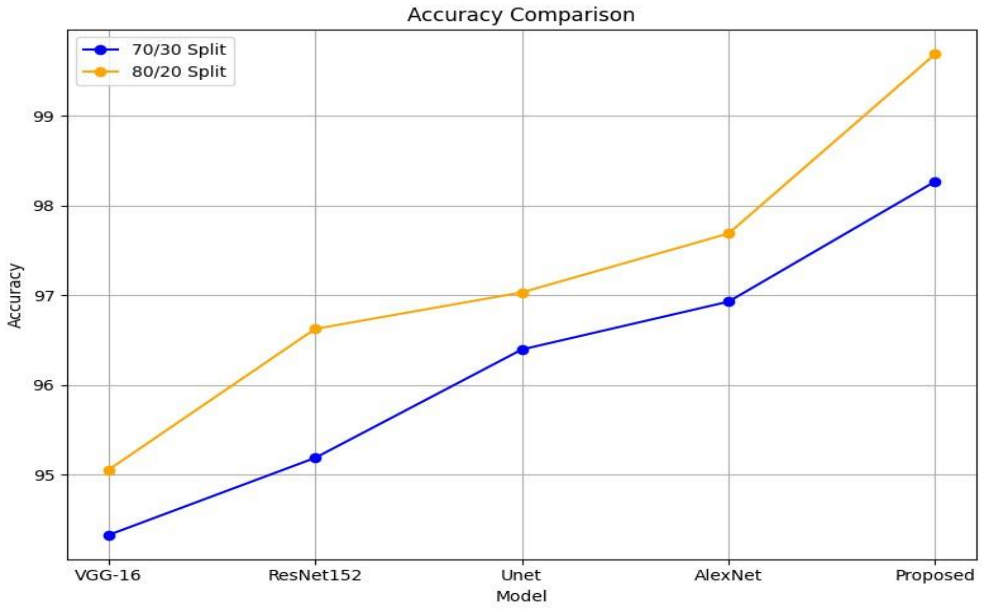

Figure 5. Performance of Accuracy

The percentage of the dependent variable's variance that can be predicted from the independent variables is shown by R^2 measure. The proposed OptiDenEffNet framework obtain the R^2 values of 99.085% for 80:20 data split and 98.442% for 70:30 split. However, the OptiDenEffNet model exhibits the highest values in both data splits than other existing models. This highest R^2score of proposed model shows that the model explaining almost all of the variance in the prediction of retinal disorders. This implies that the recommended OptiDenEffNet outperforms the other models in capturing intricate patterns in the data. The evaluation results of R^2 is shown in Figure 6.

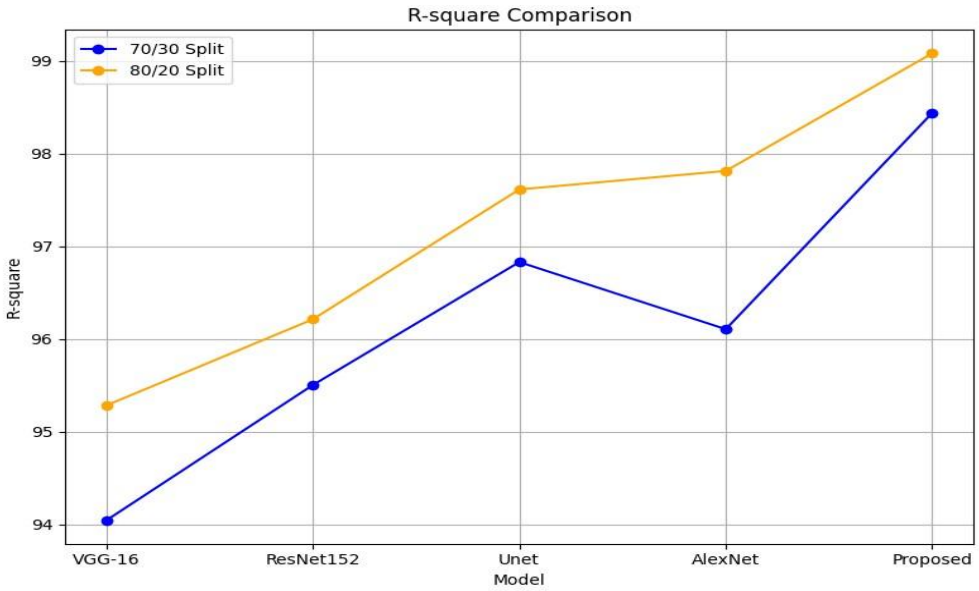

Figure 6. Performance of R-Squared

A lower RMSE value denotes higher performance. RMSE is an absolute measure of prediction error. The OptiDenEffNet model's capacity to reduce prediction errors is demonstrated by its constant lowest RMSE of 0.2456 for 70:30 data split and 0.2319 for 80:20 data split. The proposed model is noticeably superior at lowering prediction deviations when compared to other models. The lowest RMSE of proposed model indicates that the model can predict the diseases accurately. The RMSE analysis of various models is shown in Figure 7.

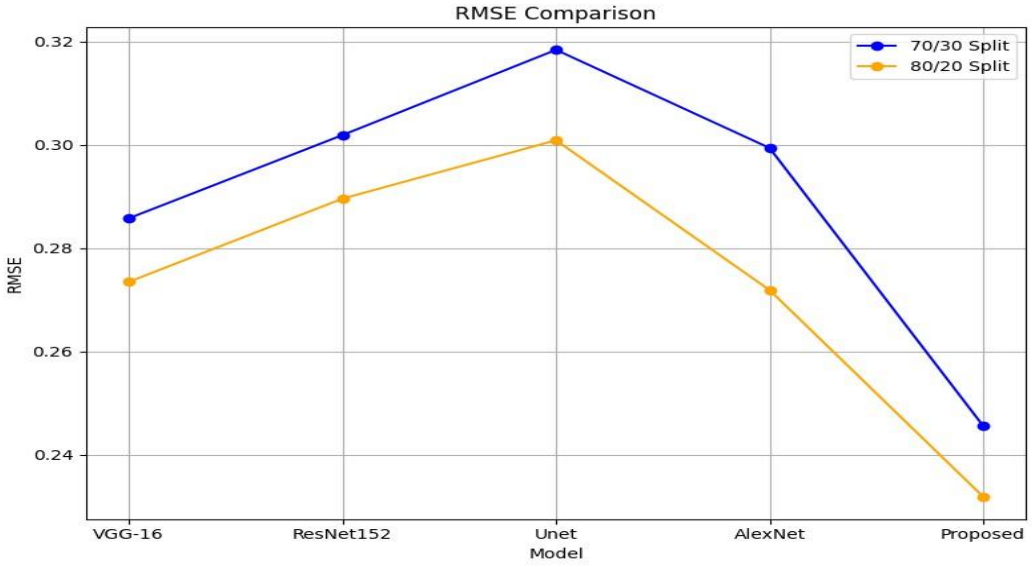

Figure 7. Performance of RMSE

MSE calculates the average squared difference between the actual and anticipated values, just like RMSE does. Once more, the proposed OptiDenEffNet model performs better than alternative models, with MSE values of 0.2418 (70:30 split) and 0.2329 (80:20 split), which are significantly lower. This indicates that the recommended model provides greater precision in the prediction of retinal disorders by more effectively reducing the size of mistakes. The evaluation of MSE results is illustrated in Figure 8.

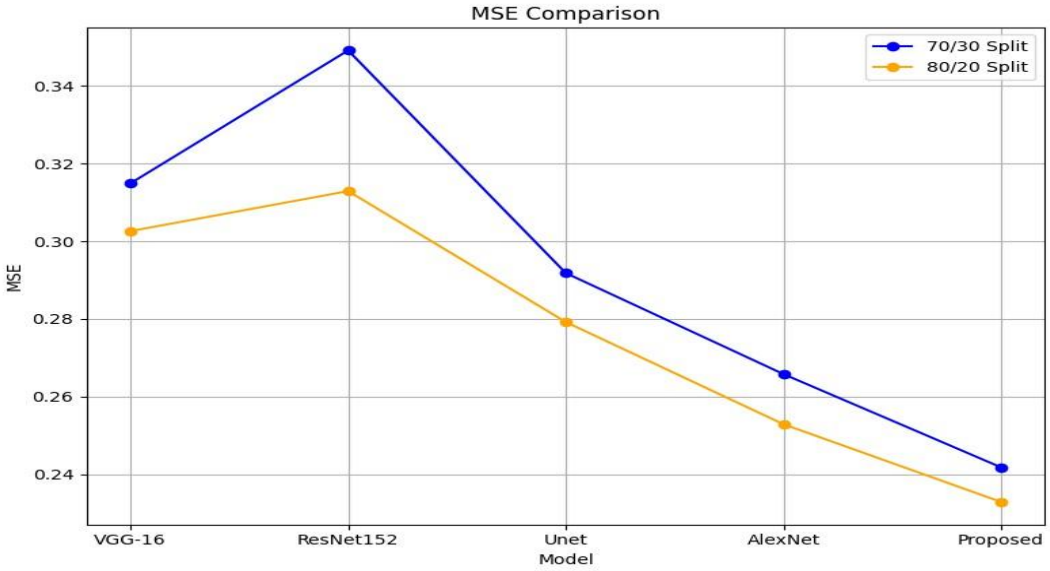

Figure 8. Performance of MSE

The prediction error is expressed as a percentage by the MAPE metric, where lower values indicate greater performance. In both splits, the proposed OptiDenEffNet technique records the lowest MAPE of 0.2214% in 70:30 split, and 0.2064% for 80:20 split). The proposed model is more effective at producing consistent predictions with little percentage-based mistakes, making it very dependable for clinical applications. In contrast, all other comparative existing models have greater MAPE values when compared to proposed model. This better MAPE result of recommended model clearly describes that the model can predict more precisely than other models. The MAPE analysis is depicted in Figure 9.

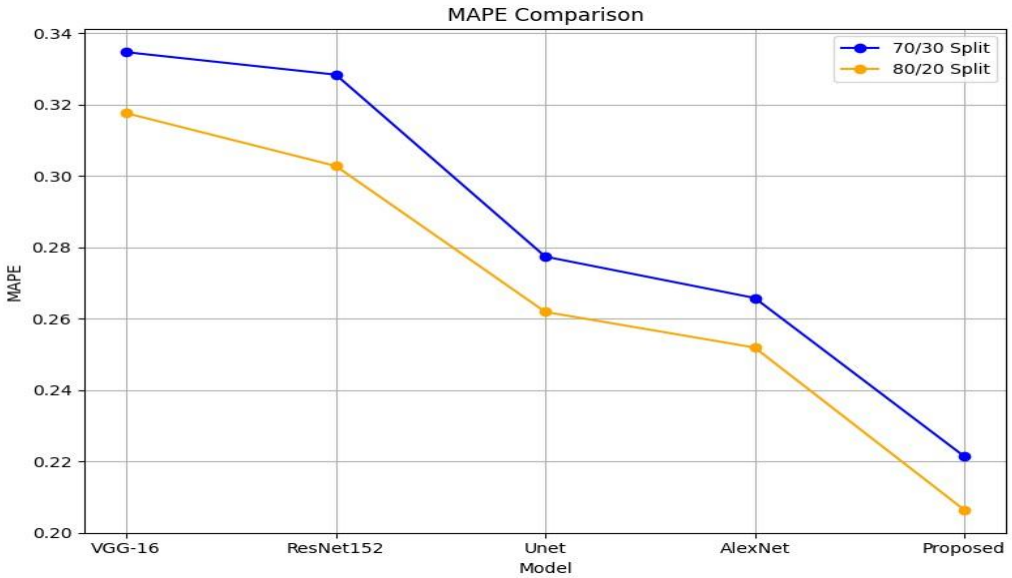

Figure 9. Performance of MAPE

The MAE calculates the average magnitude of mistakes in a series of predictions without taking direction into account. With values of 0.1958 for the 80:20 split and 0.2147 for the 70:30 split, the newly developed OptiDenEffNet method has the lowest MAE in both splits. These lowest MAE score shows that the proposed OptiDenEffNet model regularly produces predictions with smaller errors and higher accuracy than other models. The MAE evaluation results are shown in Figure 10.

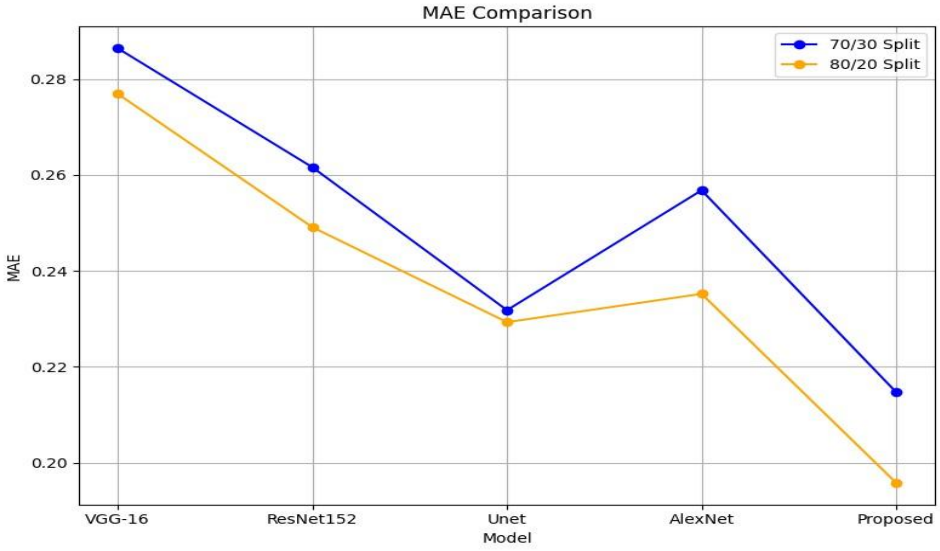

Figure 10. Performance of MAE

All major performance measures show that the proposed OptiDenEffNet model performs much better than the other current models. Its efficiency in predicting eye diseases is demonstrated by its stronger explanatory power (R-squared), reduced error rates (RMSE, MSE, MAPE, and MAE), and superior accuracy. The results shows that the proposed OptiDenEffNet framework is a potential model for ocular diagnostics because of its integration of attention mechanisms and DGRU, which improves feature extraction and prediction capabilities.

4. Conclusion

This research proposes OptiDenEffNet, a new deep learning framework, to predict various eye illnesses from data based on patient's age. The study starts with a thorough pre-processing stage that involves label encoding, data cleaning, and normalization. Discriminative deep feature representations are then extracted using recommended OptiDenEffNet model, which combines several DL blocks, and the Attention Block, which serves as a feature descriptor. Finally, a highly developed prediction model called a Discriminative Gated Recurrent Unit (DGRU) is employed. The performance of proposed model is evaluated in Python platform and model is compared with some existing models such as VGG-16, AlexNet, UNet, and ResNet 152. The proposed model is an effective approach for ophthalmic diagnostics because of its vast pre-processing and deep feature extraction methods, as well as its accuracy in predicting a range of retinal illnesses. The model constantly outperforms other methodswith accuracy of 98.269% in the 70:30 data split and 99.691% in the 80:20 data split. The outcomes unequivocally show that the developed model provides an extremely efficient automated method for identifying various retinal illnesses, eliminating the subjectivity and mistakes that could result from ophthalmologists making human diagnoses. Pre-trained models and transfer learning techniques can minimize training time and computational expenses while preserving or enhancing classification performance.

References

1. Umer, M.J.; Sharif, M.; Raza, M.; Kadry, S.J. A deep feature fusion and selection-based retinal eye disease detection from OCT images. Expert Syst. 2023, 40, e13232.
2. Fan, B., Zhang, C., Chi, J., Liang, Y., Bao, X., Cong, Y., Yu, B., Li, X. and Li, G.Y., 2022. The molecular mechanism of retina light injury focusing on damage from short wavelength light. Oxidative medicine and cellular longevity, 2022(1), p.8482149.
3. Akram A, Debnath R (2020) An automated eye disease recognition system from visual content of facial images using machine learning techniques. Turkish J Electr Eng Comput Scis 28(2):917–932
4. Sarki, R., Ahmed, K., Wang, H. and Zhang, Y., 2020. Automated detection of mild and multi-class diabetic eye diseases using deep learning. Health Information Science and Systems, 8(1), p.32.

5. Pratap T, Kokil P (2021) Efcient network selection for computer-aided cataract diagnosis under noisy environment. Comput Methods Programs Biomed 200:105927
6. Bhatwadekar, A.D., Shughoury, A., Belamkar, A. and Ciulla, T.A., 2021. Genetics of diabetic retinopathy, a leading cause of irreversible blindness in the industrialized world. Genes, 12(8), p.1200.
7. Ho, S., Kalloniatis, M. and Ly, A., 2022. Clinical decision support in primary care for better diagnosis and management of retinal disease. Clinical and Experimental Optometry, 105(6), pp.562-572.
8. Karn, P.K. and Abdulla, W.H., 2023. On machine learning in clinical interpretation of retinal diseases using oct images. Bioengineering, 10(4), p.407.
9. Sharif, N.A., 2022. Neuropathology and therapeutics addressing glaucoma, a prevalent retina-optic nerve-brain disease that causes eyesight impairment and blindness. OBM Neurobiology, 6(1), pp.1-51.
10. Zhang, R.H., Liu, Y.M., Dong, L., Li, H.Y., Li, Y.F., Zhou, W.D., Wu, H.T., Wang, Y.X. and Wei, W.B., 2022. Prevalence, years lived with disability, and time trends for 16 causes of blindness and vision impairment: findings highlight retinopathy of prematurity. Frontiers in Pediatrics, 10, p.735335.
11. Zeppieri, M., Marsili, S., Enaholo, E.S., Shuaibu, A.O., Uwagboe, N., Salati, C., Spadea, L. and Musa, M., 2023. Optical coherence tomography (OCT): a brief look at the uses and technological evolution of ophthalmology. Medicina, 59(12), p.2114.
12. Schreur, V., Larsen, M.B., Sobrin, L., Bhavsar, A.R., den Hollander, A.I., Klevering, B.J., Hoyng, C.B., de Jong, E.K., Grauslund, J. and Peto, T., 2022. Imaging diabetic retinal disease: clinical imaging requirements. Acta ophthalmologica, 100(7), pp.752-762.
13. Yoo, T.K., Choi, J.Y. and Kim, H.K., 2021. Feasibility study to improve deep learning in OCT diagnosis of rare retinal diseases with few-shot classification. Medical & biological engineering & computing, 59, pp.401-415.
14. Ong, J., Zarnegar, A., Corradetti, G., Singh, S.R. and Chhablani, J., 2022. Advances in optical coherence tomography imaging technology and techniques for choroidal and retinal disorders. Journal of Clinical Medicine, 11(17), p.5139.
15. T. Kurmann, S. Yu, P. Márquez-Neila, A. Ebneter, M. Zinkernagel, M. R. Munk, et al., Expertlevel automated biomarker identification in optical coherence tomography scans, Sci. Rep., 9 (2019), 1–9. https://doi.org/10.1038/s41598-019-49740-7
16. Choudhary, A., Ahlawat, S., Urooj, S., Pathak, N., Lay-Ekuakille, A. and Sharma, N., 2023, January. A deep learning-based framework for retinal disease classification. In Healthcare (Vol. 11, No. 2, p. 212). MDPI.
17. Khan, A., Pin, K., Aziz, A., Han, J.W. and Nam, Y., 2023. Optical coherence tomography image classification using hybrid deep learning and ant colony optimization. Sensors, 23(15), p.6706.
18. Stanojević, M., Drašković, D. and Nikolić, B., 2023. Retinal disease classification based on optical coherence tomography images using convolutional neural networks. Journal of Electronic Imaging, 32(3), pp.032004-032004.
19. Shoukat, A., Akbar, S., Hassan, S.A., Iqbal, S., Mehmood, A. and Ilyas, Q.M., 2023. Automatic diagnosis of glaucoma from retinal images using deep learning approach. Diagnostics, 13(10), p.1738.
20. Albelaihi, A. and Ibrahim, D.M., 2024. DeepDiabetic: An Identification System of Diabetic Eye Diseases Using Deep Neural Networks. IEEE Access.
21. Hemalakshmi, G.R., Murugappan, M., Sikkandar, M.Y., Begum, S.S. and Prakash, N.B., 2024. Automated retinal disease classification using hybrid transformer model (SViT) using optical coherence tomography images. Neural Computing and Applications, pp.1-18.
22. Hassan, S.A., Akbar, S. and Khan, H.U., 2024. Detection of central serous retinopathy using deep learning through retinal images. Multimedia Tools and Applications, 83(7), pp.21369-21396.

23. Zia, A., Mahum, R., Ahmad, N., Awais, M. and Alshamrani, A.M., 2024. Eye diseases detection using deep learning with BAM attention module. Multimedia Tools and Applications, 83(20), pp.59061-59084.
24. Nguyen, T.D., Le, D.T., Bum, J., Kim, S., Song, S.J. and Choo, H., 2024. Retinal disease diagnosis using deep learning on ultra-wide-field fundus images. Diagnostics, 14(1), p.105.
25. George, N., Shine, L., Ambily, N., Abraham, B. and Ramachandran, S., 2024. A two-stage CNN model for the classification and severity analysis of retinal and choroidal diseases in OCT images. International Journal of Intelligent Networks, 5, pp.10-18.
26. Ocular Disease Recognition,https://www.kaggle.com/datasets/andrewmvd/ocular-disease-recognition-odir5k?resource=downloadAccessed on September 2024.